Published in final edited form as:

Curr Biol. 2019 December 16; 29(24): 4291–4299.e4. doi:10.1016/j.cub.2019.10.027.

Activation of Kappa Opioid Receptor Regulates the Hypothermic Response to Calorie Restriction and Limits Body Weight Loss

Rigo Cintron-Colon[1], **Christopher W. Johnson**[2], **J. Rafael Montenegro-Burke**[3], **Carlos Guijas**[3], **Lila Faulhaber**[4], **Manuel Sanchez-Alavez**[5,6], **Carlos A. Aguirre**[1], **Kokila Shankar**[1], **Mona Singh**[1], **Andrea Galmozzi**[1], **Gary Siuzdak**[3,7], **Enrique Saez**[1], **Bruno Conti**[*,1,5,8]

[1]Department of Molecular Medicine, The Scripps Research Institute, La Jolla, California 92037, USA.

[2]Graduate Program in Neuroscience, University of Washington, Seattle, WA 98195, USA.

[3]Scripps Center for Metabolomics, The Scripps Research Institute, La Jolla, California 92037, USA.

[4]Department of Biochemistry, University of Washington, Seattle, WA 98195, USA.

[5]Department of Neuroscience, The Scripps Research Institute, La Jolla, California 92037, USA.

[6]Facultad de Medicina y Psicología, Universidad Autónoma de Baja California, Tijuana, 22390 México.

[7]Departments of Chemistry, Molecular and Computational Biology, The Scripps Research Institute, La Jolla, California 92037, USA.

[8]Department of Biochemistry and Biophysics, Stockholm University, S-106 91 Stockholm, Sweden

SUMMARY

Mammals maintain a nearly constant core body temperature (T_b) by balancing heat production and heat dissipation. This comes at a high metabolic cost which is sustainable if adequate calorie intake is maintained. When nutrients are scarce or experimentally reduced such as during calorie restriction (CR), endotherms can reduce energy expenditure by lowering T_b [1–6]. This adaptive response conserves energy, limiting the loss of body weight due to low calorie intake [7–10]. Here we show that this response is regulated by the kappa opioid receptor (KOR). CR associated with increased hypothalamic levels of the endogenous opioid leu-enkephalin; which is derived from the KOR agonist precursor, dynorphin [11]. Pharmacological inhibition of KOR, but not of the delta or the mu opioid receptor subtypes, fully blocked CR-induced hypothermia and increased weight loss during CR independently of calorie intake. Similar results were seen with diet-induced obese mice subjected to CR. In contrast, inhibiting KOR did not change T_b in animals fed *ad libitum*.

[*]Lead Contact: Phone: 858-784-9069. bconti@scripps.edu.

AUTHOR CONTRIBUTIONS

Conceptualization and methodology: R.C.-C., A.G., and B.C.; Data analysis and curation: R.C.-C., C.W.J. and J.R.M.-B.; Investigation: R.C.-C., C.W.J., J.R.M.-B., C.G., M.S.-A., C.A.A., M.S., K.S., L.F., and A.G.; Writing – Review & Editing: R.C.-C., C.W.J., J.R.M.-B, E.S. and B.C. with contributions from of all other authors; Supervision and funding acquisition: E.S, G.S. and B.C.

DECLARATION OF INTERESTS

The authors declare no competing interests.

Chemogenetic inhibition of KOR neurons in the hypothalamic preoptic area reduced the CR-induced hypothermia, while chemogenetic activation of prodynorphin-expressing neurons in the arcuate or the parabrachial nuclei lowered T_b. These data indicate that KOR signaling is a pivotal regulator of energy homeostasis and can affect body weight during dieting by modulating T_b and energy expenditure.

Graphical Abstract

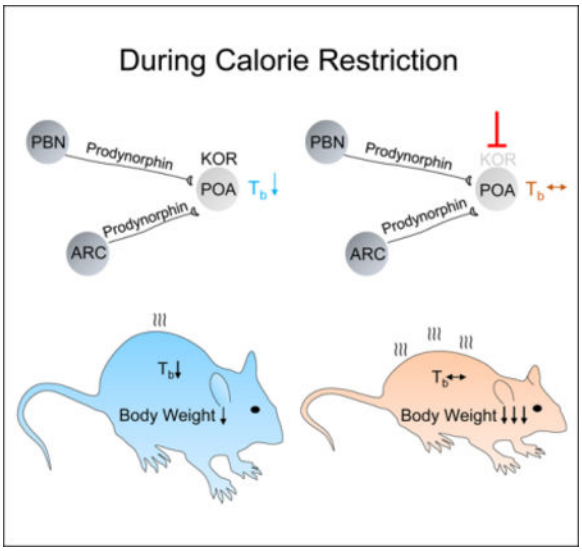

eTOC blurb

During calorie restriction endotherms lower core body temperature to limit energy expenditure and weight loss. Cintron-Colon *et al.* show in mice that this response is regulated centrally by prodynorphin and by kappa opioid receptor (KOR) neurons and that pharmacological inhibition of KOR during dieting prevents hypothermia, increasing weight loss.

Keywords

Kappa Opioid Receptor; Dynorphin; Body Weight; Body Temperature; Hypothermia; Calorie Restriction; Dieting; Energy Expenditure; Energy Homeostasis

RESULTS and DISCUSSION

Mice housed at 22 °C and subjected to gradual reduction of calorie intake with food provided in bolus once a day develop a hypothermic response with a transient and circadian T_b reduction of up to 10 °C as the CR regimen progresses. This T_b reduction starts ~7 hr after the daily meal is consumed between ZT11 to ZT14 and it continues until reaching its lowest point by ZT1 to ZT3 (Figure 1A and B). On average the T_b is below 34°C for ~16 hr (ZT18 to ZT10). Then, mice gradually increase their T_b reaching its normal value and they engage in food consumption provided between ZT11 to ZT12. Calorie restricted mice learn to anticipate the feeding time. As a result, animals on CR increase locomotor activity to engage in exploratory behavior after ZT3, also coinciding with the increase in T_b (Figure

1B). Under these conditions, mice lose 0.5% to 2.5% of their body weight daily until they plateau with a total loss of 19% of body weight relative to mice fed *ad libitum* (Figure 1C and D).

We recently designed an experimental protocol to determine which metabolomic changes occurring during CR are due to the hypothermic response rather than due to a reduction in calorie intake (C.G., J.R.M.-B., R.C.-C., X.D. Almenara, M.S.-A., C. A., K.S., E.L.W. Majumder, E. Billings, G.S., B.C., unpublished observations)) (Figure S1A). Experiments were carried out on plasma and on tissue from the hypothalamus, a brain region that regulates both nutrient and temperature homeostasis [12–15]. We found that the hypothalamic but not the plasma level of the endogenous opioid peptide leucine-enkephalin (LENK) increased steadily during a 24-hr period in CR (Figure S1B). Since opioids and their receptors are known regulators of energy homeostasis [16–22] and body weight [23–26], we hypothesized that the opioid system could also modulate the hypothermic response to CR.

To test this hypothesis, we evaluated the effects of different opioid receptors modulators on hypothermia development and on body weight loss during CR. We targeted pharmacologically the three known classes of opioid receptors, mu (μ or MOR), delta (δ or DOR) and kappa (κ or KOR), which are expressed throughout the brain including the hypothalamus [27, 28]. We used nonselective antagonists as well as selective antagonists with distinct receptor affinities (Table S1). These antagonists were injected intraperitoneally as they are known to cross the blood brain barrier to act in the CNS [29–36].

Naloxone, a nonselective antagonist with higher affinity for MOR than the other receptors did not prevent the extent of the fall in T_b upon CR at either of two doses tested (5 and10 mg/kg) (Figure 2A and 2B and C). Likewise, Naloxonazine, a selective MOR antagonist had no effect (Figure 2A and 2D and E), suggesting that MOR is unlikely to be involved in the regulation of the hypothermic response to CR. The possible involvement of DOR was tested with Naltrindole, a specific antagonist of both the δ_1 and the δ_2 subtypes, and with BNTX and Naltriben, which are specific for δ_1 and δ_2, respectively. Naltrindole did not prevent but rather prolonged CR-induced hypothermia by ~5 hr compared to vehicle-treated mice (Figure 2A, 2F and G). BNTX prevented the fall in T_b upon CR only mildly (16.8%) (Figure 2A and 2H and I) and Naltriben was even weaker with 5% reduction at the highest dose tested (10 mg/kg) (Figure 2A and 2J and K). The role of the KOR was assessed with the selective antagonist Dippa Hydrochloride (DH). DH prevented CR-induced hypothermia by 72.2% and 51.1% when tested at 5 and 10 mg/kg, respectively (Figure 2A, 2L and 2M). Together, these data indicate that the KOR is the main regulator of the hypothermic response to CR.

KOR is the most abundant opioid receptor in the hypothalamus and its strongest endogenous ligands are dynorphins from which Leu-enkephalin is derived by proteolytic cleavage [11]. Although dynorphins are too large to be detected with the metabolomic approach used, they are known to increase during fasting and to lower T_b when administered intracerebroventricularly to animals fed *ad libitum* [21, 37, 38]. This suggested that these opioid peptides may be regulating the hypothermic response to CR. We tested this

hypothesis by measuring the ability of prodynorphin (Pdyn)-expressing neurons to modulate T_b. We used a chemogenetic approach to activate Pdyn-expressing neurons in the arcuate (ARC) or the parabrachial nucleus (PBN). Neurons in the ARC and PBN regulate appetite and energy balance and may contribute to temperature homeostasis as a means to conserve energy when nutrients are scarce [15, 22, 39–41]. The PBN was already recognized to contribute to temperature homeostasis [42–45]. Both regions project to the hypothalamic preoptic area (POA), which is a pivotal regulator of temperature homeostasis [46–48].

To selectively activate Pdyn neurons, we used mice that have Cre recombinase targeted to the *Pdyn* locus ($Pdyn^{Cre:GFP}$ mice) or the *Oprk* locus that encodes KOR ($Oprk^{Cre}$ mice) and injected AAV1-DIO-hM3Dq:mCherry into either the PBN or the ARC. Mice fed *ad libitum* were then either injected with CNO (to activate the designer receptor, hM3Dq) or saline. Using this strategy, activation of Pdyn neurons in either the ARC or the PBN decreased the T_b of the mice (Figure 3A–D). Likewise, activation of neurons in the POA that express KOR also decreased T_b (hM3Dq; Figure 3E and F). Conversely, chemogenetic inhibition of KOR neurons in the POA by injection of AAV that carries a Cre-dependent inhibitory receptor (AAV-DIO-hM4Di:mCherry) reduced the effect of CR on T_b (Figure 3G and H) but had no effect on mice fed *ad libitum* (hM4Di; Figure 3E). Systemic antagonism of KOR during AL did not affect T_b (Figure S2). These data suggest that dynorphin, whose levels are elevated during CR, regulates T_b via KOR activation in the POA [37].

By lowering energy expenditure, the hypothermic response to CR limits body weight loss. Since this appears to require KOR, we measured the effects that pharmacological blockade of KOR with DH has on body weight. First, we measured the effects of DH (5 mg/kg) in lean mice (body weight of mice a day before treatment started: vehicle, 24.16 ± 0.36 g vs DH, 24.19 ± 0.31 g; $t(10) = 0.0529$, $p = 0.9588$) subjected to 6 weeks of 50% CR. These mice had adapted to the new dietary regimen and their body weight loss had plateaued. Relative to vehicle-treated animals, mice receiving DH administered daily for 5 consecutive days did not develop a hypothermic response, showed increased energy expenditure and underwent a further 6% reduction of body weight (day 3: vehicle, 24.27 ± 0.47 g vs DH, 22.70 ± 0.56 g; $t(70) = 2.893$, $p = 0.0350$) which was evident starting at day 3 of treatment (Figure 4A–C). These effects disappeared once DH treatment was stopped. Next, we measured the effects of DH treatment on diet-induced obese (DIO) mice subject to 33.6% CR (Methods and Figure S3). Before DH treatment started, the vehicle group did not differ in body weight from the DH group (vehicle, 48.68 ± 1.53 g vs DH, 47.8 ± 0.91 g; $t(10) = 0.4954$, $p = 0.6310$). DH treatment lowered the hypothermic response to CR and induced greater body weight loss (Figure 4D and E). These effects were evident starting at day 1 with a significant body weight loss in mice receiving DH (8%) relative to vehicle (3.64%) and reached a cumulative body weight reduction by the last day of DH + CR treatment of 13% vs. 8% seen in vehicle + CR treated mice (Figure 4E). After 3 days of DH treatment, the fasting glucose level of obese animals was reduced by ~18% in comparison to vehicle-treated animals (two-tailed unpaired t test, $t(10) = 3.431$, $P= 0.0064$). These data are consistent with previous findings showing that genetic deletion of *Oprk* promotes energy expenditure and weight loss when reared on a high-fat diet [23].

Our chemogenetic experiments demonstrated that these effects are mediated, at least in part, centrally by KOR in the POA and by dynorphin neurons in the ARC or the PBN. The ARC regulates feeding and neuroendocrine functions while the Pdyn neurons of the PBN are recognized to be part of a neural circuit with afferents from the skin [42, 45]. Both regions project to the POA and, as our data indicate, they can be modulated by the opioid system to regulate T_b in response to CR, with the PBN having stronger effects than the ARC.

The opioid system was previously shown to regulate feeding or body temperature in fever, hypoxia or heat stroke (reviewed in [49]). Specifically, activation of MOR and KOR produced hyperthermia or hypothermia, respectively, while DOR contributed to both by regulating the function of neurons in the POA including warm-sensitive neurons [29, 50–70]. Here we showed that the opioid system helps to maintain homeostasis by integrating energy intake and expenditure. These effects were only seen when animals were subject to CR, as DH did not alter T_b of animals fed AL, and they were mediated by the KOR but not by other opioid receptors. This suggests that a system comprising the KOR and neurons in the ARC, the PBN and the POA may have specifically evolved to save energy promoting survival when nutrients are scarce. An important feature of this mechanism is that it reduces body weight loss when calorie intake is low and thus may limit body weight control during dieting [9, 10, 71–73]. Since DH was active on lean as well as on diet-induced obese mice, further pharmacological and translational studies may determine whether KOR antagonists could be used in combination with diet to facilitate body weight loss in obese individuals.

STAR METHODS

LEAD CONTACT AND MATHERIALS AVAILABILITY

Further information and requests for reagents may be directed to and will be effectuated by the Lead Contact, Bruno Conti (bconti@scripps.edu).

This study did not generate new unique reagents.

EXPERIMENTAL MODEL AND SUBJECT DETAILS

All experiments were performed in accordance with National Institutes of Health Guide for the Care and Use of Laboratory Animals and with approval from the Scripps Research Institute and the University of Washington Animal Care and Use Committee.

Mice and husbandry: Female C57BL/6 mice (4 to 7 months old) were used for the metabolomics experiments. All pharmacology experiments were performed with C57BL/6 male mice (4 to 7 months old). Animals were singly caged with 12:12 h light:dark (lights on 11:00 am; Zeitgeber Time 12 or ZT12) at a controlled ambient temperature (T_a) of 22.0 ± 0.5 °C. Water was available AL during CR experiments. Normal Chow: (Lab Diet 5053 Irradiated Pico Lab containing 3.41 kcal/g, 20.0% protein, 52.9% carbohydrates, 10.6% fat, 4.7% crude fiber and 6.1% ash) was provided AL or restricted during the CR experiments as specified. High Fat Diet: (Research Diets D12492 containing 5.21 kcal/g, 20% kcal protein, 60% kcal fat and 20% kcal carbohydrate) was provided AL starting at 3 months of age and restricted during CR experiments only at five months of age.

The Pdyn-Cre:GFP mice were generated in the Palmiter laboratory at University of Washington. Briefly, the 5' and 3' arms (each 3.2–3.5 kb) for an *Pdyn* targeting construct were amplified by PCR using Phusion Polymerase (New England Biolabs) and cloned into polylinkers of a targeting construct that contained an frt-flanked Sv40Neo with 3 polyA sites for positive selection, an attenuated Cre:GFP fusion protein with a no nuclear localization signal, non-optimal initiation codon and 3' a untranslated region/polyadenylation sequence from the mouse *Myc* gene to hasten degradation, and HSV thymidine kinase and *Pgk*-diphtheria toxin A chain genes for negative selection. The end result is that the Cre:GFP gene is inserted just 5' of the normal initiation codon for *Pdyn*. The construct was electroporated into C57BL/6 ES cells; correct targeting was determined by Southern blot of DNA digested with *SSp*I using a probe downstream of the 3' arm of the targeting construct. Of 93 clones analyzed, 26 were correctly targeted. Several clones were injected into blastocysts from C57BL/6 mice and one of them gave a high-percentage chimera that was bred with *Gt(ROSA)26Sor-FLP* recombinase mice to remove the frt-Sv40Neo cassette. The mice were then continuously backcrossed to C57BL/6 mice.

The Oprk-Cre mice were provided by the Chavkin laboratory at University of Washington and originally generated by Sarah Ross [74].

Metabolomics: The hypothalamus of mice subjected to *ad libitum* or 50% CR was collected for untargeted metabolomics analysis. Calorie restricted animals were divided into three groups for tissue collection. A 24 h period of calorie restriction-induced hypothermia was divided into three arbitrary timepoints denominated Onset (O), representing the time-point before the hypothermic response, Maintenance (M), representing the lowest T_b of the 24 hours period, and Termination (T), representing the period post hypothermia before food was provided. The hypothalamus of AL animals was collected at the time of Maintenance in respect to CR animals. Metabolite extraction from hypothalamus sections was performed as previously described [75]. Briefly, 10–30 mg of tissue was weighed and 0.6 mL of cold methanol/water (4:1, v/v) were added per 10 mg of tissue. Homogenization was performed by adding glass beads to the samples in a homogenizer and sonication in an ice-cold bath for 10 minutes. The samples were then transferred to another tube and rinsed with additional 200 mL of methanol/water (4:1, v/v) followed by incubation −20 °C for 60 minutes to all ow protein precipitation. Insoluble proteins were pelleted by centrifugation at 16000 × g for 15 minutes at 4 °C. The supernatants were transferred to another tube and dried down in a vacuum concentrator. Dry metabolite extracts were stored at −80 °C and were reconstituted in ace tonitrile/water (1:1, v/v), vortexed for 1 minute, sonicated for 15 minutes and centrifuged at 16,000 × g and 4 °C for 15 minutes to remove insoluble debris and transferred to LC glass vials prior to LC-MS analysis. Acetonitrile/water volume was adjusted using the initial mass of tissue for each sample to maintain tissue relative concentrations equal across all samples.

LC-MS analysis was performed on a I-class UPLC system coupled with a Synapt G2-S*i* mass spectrometer via an electrospray ionization (ESI) source from Waters. The positive-mode (+) ESI conditions were as follows: capillary, +3.00 kV; sampling cone, 40 V; source temperature, 100°C; desolvation temperature, 250°C; desolvation gas flow, 600 L/hr; and cone gas flow, 50 L/hr, respectively. Leucine–enkephalin (*m/z* 556.2771) was used for lock

mass correction. Liquid chromatography was performed with A= water + 0.1% formic acid and B= acetonitrile + 0.1% formic acid. Waters ACQUITY UPLC BEH C18 column (1.7 μm, 2.1 mm × 100 mm) was used at a flow rate of 400 μL/min. Initially, the mobile phase composition consisted of 1% B and held for 1 min after injection and its composition was increased to 99% B over 8 min and held for 2 min. The injection volume was 2 μL. For identification purposes, putative molecules of interest were fragmented at 3 different collision energies (10, 20 and 40 eV).

LC-MS data were converted to mzXML files using MSConvert Software (ProteoWizard 3.0). The mzXML files were uploaded to XCMS Online web platform for data processing (https://xcmsonline.scripps.edu) including peak detection, retention time correction, profile alignment, and isotope annotation [76]. Data were processed using both pair-wise and multigroup comparison, and the parameter settings were as follows: centWave for feature detection ($\Delta\ m/z$ = 15 ppm, minimum peak width = 2 s, and maximum peak width = 25 s); obiwarp settings for retention time correction (profStep = 0.5); and parameters for chromatogram alignment, including mzwid = 0.01, minfrac = 0.5, and bw = 2. The relative quantification of metabolite features was based on extracted ion chromatogram areas. Paired parametric t-test and one-way ANOVA (post hoc Tukey test) were used to test the variation pattern of metabolite features between and across samples. The results output, including EICs, pairwise/multigroup cloud plot, multidimensional scaling plots, and principle components were exported directly from XCMS Online. Generally, the numbers of total pairwise comparison features and significantly altered features (statistically defined as p value < 0.01, including both upregulated and downregulated features) were reported in this study. Reported metabolites are level 1 according to MSI standards [77, 78].

Pharmacology: All opioid receptor antagonists were administered i.p. Naloxone hydrochloride (Tocris, 0599), Naloxonazine dihydrochloride (Tocris, 0591) and Naltrindole hydrochloride (Tocris, 0740) were dissolved in saline. BNTX maleate (Tocris, 0899), Naltriben mesylate (Tocris, 0892) and DIPPA hydrochloride (Tocris, 0794) were dissolved in castor oil:EtOH:saline (1:1:18).

Viruses and stereotactic injections: Mice under 6 months of age received bilateral injections in the PBN or ARC and unilateral injection in the POA of Cre-dependent hM3Dq:YFP (AAV1-Ef1a-DIO-hM3Dq:YFP); 400 nl of virus (~10^9 particles per μl) was delivered to each targeted injection site. Viruses were prepared at the University of Washington [79]. Surgeries were performed aseptically under constant infusion of isoflurane (2% isoflurane/O_2) while head-fixed to a stereotaxic frame. Targeted injections were performed using a Neurostar Drill and Injection Robot system (Tubingen, Germany) with a 33-Ga needle (NanoFil NF33BL). Viruses were injected bilaterally into the PBN (with respect to Bregma, anteroposterior (AP): −4.60 mm; mediolateral (ML): ± 1.30 mm; dorsoventral (DV): 3.40 mm), the ARC (AP: −1.25 mm, ML: ± 0.30 mm, DV: 5.80 mm) and medially into POA (AP: +0.45 mm; ML: 0.00 mm; DV: 4.65 mm) over 5 min, and injectors were left in place for 10 min before being slowly removed.

Calorie-Restriction Treatments: Figure 2 and Figure 4A–C, animals were on a 50% CR regimen and treatments were started once the daily hypothermic response [80] (T_b < 34°C

for approximately 6–8 hours) was consistently established, 14 days after the CR protocol was started. Food was provided daily, during a one-hour window before the lights were turned off (ZT12). All mice ate the entire amount of food provided during CR experiments. Antagonist injections were performed 5 to 6 hours before the hypothermic response (ZT18-ZT19).

Figure 3G, baseline food intake was measured for 3 days prior to start the experiment. Mice were then given 50% of baseline food intake for two days. Half the mice received CNO in their drinking water (5 mg/kg/day) and half received normal drinking water. After a week recovery with *ad libitum* food, mice were again given 50% of baseline food intake with the CNO and control groups reversed. The data presented was calculated as a change from baseline $T_{b.}$

Figure 4D–E, animals were on a 33.6% CR as determined from experiments on AL and CR with continuous Dippa Hydrochloride (DH) treatment to determine the appropriate food intake upon high-fat diet, as previous studies have shown the effects of kappa opioid receptor antagonism on food intake reduction in obese Zucker and diet-induced obese rats [81]. Animals receiving DH treatment either *ad libitum* or on 75% CR progressively reduced their food intake until reaching a low but constant intake between 30.56% to 34.89% in the last 2 days out of 5 days on treatment (Figure S3). These percentages from the last two days for AL and CR on DH treatment were used to calculate the given CR percentage of 33.6%. Using this average, DIO mice ate the entire amount of food provided daily, thus uncoupling the effects of DH treatment on food intake reduction and energy expenditure for proper body weight loss analysis. DH or vehicle treatment in combination with CR started at the same time over three consecutive days. On the fourth day, animals returned to AL feeding of high-fat diet.

Acute stimulation of neurons: Figure 3A, 3C and 3E, CNO (1.0 mg/kg) or saline (10 μl/g BW) was administered intraperitoneally 1 hr after the start of the dark cycle (ZT13) during AL feeding. The data presented was calculated as a change from baseline $T_{b.}$

Physiological recordings: Core body temperature (T_b) was recorded using a surgically implanted telemetry system into the peritoneal cavity as previously described [82] (G2 E-Mitters, Starr Life Sciences or TA10TA-F10, Data Sciences, Inc.) and analyzed using the software provided (VitalView for the G2 E-Mitters).

Reduction of the Hypothermic Response to CR: The reduction of the hypothermic response to CR was calculated by measuring the area under the curve (AUC) of the temperature profile with GraphPad Prism 7 (San Diego, CA), assigning as baseline the hour (−1) and the T_b (≥ 34°C) before treatment for each individual subject. The group average for the control (vehicle) group was calculated and used to determine the percentage by which each individual antagonist reduced the hypothermic response to CR in every treated animal with the corresponding opioid receptor antagonist. From these individual percentages, a group mean was calculated and reported in Figure 2A.

Body Weight Loss: Percentage body weight loss was calculated from either the day before the treatment was started (Figure 4B and 4E), from *ad libitum* feeding (Figure 1D), or day to day during calorie restriction (Figure 1C).

Fasting Glucose: Animals on *ad libitum* feeding of high fat diet were fasted for 16 h at ZT19 and glucose measurements were taken at ZT11. Animals on three days CR of high fat diet and DH treatment were also fasted for ~16 h as they actually completed their meals by ZT17 to ZT19 and glucose was measured at ZT11. *Ad libitum* measurements were used for normalization, presenting the change upon treatment during CR.

QUANTIFICATION AND STATISTICAL ANALYSIS

Microsoft excel and GraphPad Prism 7 were used for figure generation and data analysis; statistical details are in figure legends.

DATA ON CODE AVAILABILITY

Metabolomics data will be available at XCMS Online, all other raw data presented in this paper is available upon request.

Supplementary Material

Refer to Web version on PubMed Central for supplementary material.

ACKNOWLEDGEMENTS

This work was supported by The National Institute of Health, GM113894 (B.C.) and RC2 DK114785 (E.S.). R01 GM114368-03, P30 MH062261-17, P01 DA026146-02 and the NIH Cloud Credits Model Pilot, a component of the NIH Big Data to Knowledge (BD2K) program (G.S.). R.C.-C. was supported by the Skaggs Graduate School of Chemical and Biological Sciences and ARCS Foundation. The authors would like to thank Richard Palmiter for helpful comments on the manuscript.

References

1. Speakman JR, and Mitchell SE (2011). Caloric restriction. Mol Aspects Med 32, 159–221. [PubMed: 21840335]
2. Soare A, Cangemi R, Omodei D, Holloszy JO, and Fontana L (2011). Long-term calorie restriction, but not endurance exercise, lowers core body temperature in humans. Aging (Albany NY) 3, 374–379. [PubMed: 21483032]
3. Ruf T, and Geiser F (2015). Daily torpor and hibernation in birds and mammals. Biol Rev Camb Philos Soc 90, 891–926. [PubMed: 25123049]
4. Cintron-Colon R, Sanchez-Alavez M, Nguyen W, Mori S, Gonzalez-Rivera R, Lien T, Bartfai T, Aid S, Francois JC, Holzenberger M, et al. (2017). Insulin-like growth factor 1 receptor regulates hypothermia during calorie restriction. Proc Natl Acad Sci U S A 114, 9731–9736. [PubMed: 28827363]
5. Carrillo AE, and Flouris AD (2011). Caloric restriction and longevity: effects of reduced body temperature. Ageing Res Rev 10, 153–162. [PubMed: 20969980]
6. Mitchell SE, Delville C, Konstantopedos P, Derous D, Green CL, Chen L, Han JD, Wang Y, Promislow DE, Douglas A, et al. (2015). The effects of graded levels of calorie restriction: III. Impact of short term calorie and protein restriction on mean daily body temperature and torpor use in the C57BL/6 mouse. Oncotarget 6, 18314–18337. [PubMed: 26286956]

7. Song X, and Geiser F (1997). Daily torpor and energy expenditure in Sminthopsis macroura: interactions between food and water availability and temperature. Physiol Zool 70, 331–337. [PubMed: 9231407]
8. Schubert KA, Boerema AS, Vaanholt LM, de Boer SF, Strijkstra AM, and Daan S (2010). Daily torpor in mice: high foraging costs trigger energy-saving hypothermia. Biol Lett 6, 132–135. [PubMed: 19710051]
9. Mitchell SE, Tang Z, Kerbois C, Delville C, Konstantopedos P, Bruel A, Derous D, Green C, Aspden RM, Goodyear SR, et al. (2015). The effects of graded levels of calorie restriction: I. impact of short term calorie and protein restriction on body composition in the C57BL/6 mouse. Oncotarget 6, 15902–15930. [PubMed: 26079539]
10. Mitchell SE, Tang Z, Kerbois C, Delville C, Derous D, Green CL, Wang Y, Han JJ, Chen L, Douglas A, et al. (2017). The effects of graded levels of calorie restriction: VIII. Impact of short term calorie and protein restriction on basal metabolic rate in the C57BL/6 mouse. Oncotarget 8, 17453–17474. [PubMed: 28193912]
11. Ner J, and Silberring J (2013). Dynorphin convertases and their functions in CNS. Curr Pharm Des 19, 1043–1051. [PubMed: 23016689]
12. Zhao ZD, Yang WZ, Gao C, Fu X, Zhang W, Zhou Q, Chen W, Ni X, Lin JK, Yang J, et al. (2017). A hypothalamic circuit that controls body temperature. Proc Natl Acad Sci U S A 114, 2042–2047. [PubMed: 28053227]
13. Tabarean I, Morrison B, Marcondes MC, Bartfai T, and Conti B (2010). Hypothalamic and dietary control of temperature-mediated longevity. Ageing Res Rev 9, 41–50. [PubMed: 19631766]
14. Bartfai T, and Conti B (2012). Molecules affecting hypothalamic control of core body temperature in response to calorie intake. Frontiers in genetics 3, 184. [PubMed: 23097647]
15. Waterson MJ, and Horvath TL (2015). Neuronal Regulation of Energy Homeostasis: Beyond the Hypothalamus and Feeding. Cell Metab 22, 962–970. [PubMed: 26603190]
16. Ardianto C, Yonemochi N, Yamamoto S, Yang L, Takenoya F, Shioda S, Nagase H, Ikeda H, and Kamei J (2016). Opioid systems in the lateral hypothalamus regulate feeding behavior through orexin and GABA neurons. Neuroscience 320, 183–193. [PubMed: 26855191]
17. Li D, Olszewski PK, Shi Q, Grace MK, Billington CJ, Kotz CM, and Levine AS (2006). Effect of opioid receptor ligands injected into the rostral lateral hypothalamus on c-fos and feeding behavior. Brain Res 1096, 120–124. [PubMed: 16716266]
18. Papaleo F, Kieffer BL, Tabarin A, and Contarino A (2007). Decreased motivation to eat in mu-opioid receptor-deficient mice. Eur J Neurosci 25, 3398–3405. [PubMed: 17553008]
19. Romero-Pico A, Vazquez MJ, Gonzalez-Touceda D, Folgueira C, Skibicka KP, Alvarez-Crespo M, Van Gestel MA, Velasquez DA, Schwarzer C, Herzog H, et al. (2013). Hypothalamic kappa-opioid receptor modulates the orexigenic effect of ghrelin. Neuropsychopharmacology 38, 1296–1307. [PubMed: 23348063]
20. Wolinsky TD, Carr KD, Hiller JM, and Simon EJ (1994). Effects of chronic food restriction on mu and kappa opioid binding in rat forebrain: a quantitative autoradiographic study. Brain Res 656, 274–280. [PubMed: 7820587]
21. Berman Y, Devi L, and Carr KD (1994). Effects of chronic food restriction on prodynorphin-derived peptides in rat brain regions. Brain Res 664, 49–53. [PubMed: 7895045]
22. Kim EM, Welch CC, Grace MK, Billington CJ, and Levine AS (1996). Chronic food restriction and acute food deprivation decrease mRNA levels of opioid peptides in arcuate nucleus. Am J Physiol 270, R1019–1024. [PubMed: 8928900]
23. Czyzyk TA, Nogueiras R, Lockwood JF, McKinzie JH, Coskun T, Pintar JE, Hammond C, Tschop MH, and Statnick MA (2010). kappa-Opioid receptors control the metabolic response to a high-energy diet in mice. FASEB J 24, 1151–1159. [PubMed: 19917675]
24. Czyzyk TA, Romero-Pico A, Pintar J, McKinzie JH, Tschop MH, Statnick MA, and Nogueiras R (2012). Mice lacking delta-opioid receptors resist the development of diet-induced obesity. FASEB J 26, 3483–3492. [PubMed: 22593549]
25. Tabarin A, Diz-Chaves Y, Carmona Mdel C, Catargi B, Zorrilla EP, Roberts AJ, Coscina DV, Rousset S, Redonnet A, Parker GC, et al. (2005). Resistance to diet-induced obesity in mu-opioid

receptor-deficient mice: evidence for a “thrifty gene”. Diabetes 54, 3510–3516. [PubMed: 16306369]

26. Greenway FL, Fujioka K, Plodkowski RA, Mudaliar S, Guttadauria M, Erickson J, Kim DD, Dunayevich E, and Group C-IS (2010). Effect of naltrexone plus bupropion on weight loss in overweight and obese adults (COR-I): a multicentre, randomised, double-blind, placebo-controlled, phase 3 trial. Lancet 376, 595–605. [PubMed: 20673995]
27. Le Merrer J, Becker JA, Befort K, and Kieffer BL (2009). Reward processing by the opioid system in the brain. Physiol Rev 89, 1379–1412. [PubMed: 19789384]
28. Mansour A, Fox CA, Akil H, and Watson SJ (1995). Opioid-receptor mRNA expression in the rat CNS: anatomical and functional implications. Trends Neurosci 18, 22–29. [PubMed: 7535487]
29. Baker AK, and Meert TF (2002). Functional effects of systemically administered agonists and antagonists of mu, delta, and kappa opioid receptor subtypes on body temperature in mice. J Pharmacol Exp Ther 302, 1253–1264. [PubMed: 12183687]
30. Lutz PE, and Kieffer BL (2013). Opioid receptors: distinct roles in mood disorders. Trends Neurosci 36, 195–206. [PubMed: 23219016]
31. Morse M, Sun H, Tran E, Levenson R, and Fang Y (2013). Label-free integrative pharmacology on-target of opioid ligands at the opioid receptor family. BMC Pharmacol Toxicol 14, 17. [PubMed: 23497702]
32. Kim JH, and Richardson R (2009). The effect of the mu-opioid receptor antagonist naloxone on extinction of conditioned fear in the developing rat. Learn Mem 16, 161166.
33. Smith CM, Walker LL, Leeboonngam T, McKinley MJ, Denton DA, and Lawrence AJ (2016). Endogenous central amygdala mu-opioid receptor signaling promotes sodium appetite in mice. Proc Natl Acad Sci U S A 113, 13893–13898. [PubMed: 27849613]
34. Rawls SM, Hewson JM, Inan S, and Cowan A (2005). Brain delta2 opioid receptors mediate SNC-80-evoked hypothermia in rats. Brain Res 1049, 61–69. [PubMed: 15936000]
35. Carr GV, and Lucki I (2010). Comparison of the kappa-opioid receptor antagonist DIPPA in tests of anxiety-like behavior between Wistar Kyoto and Sprague Dawley rats. Psychopharmacology (Berl) 210, 295–302. [PubMed: 20369354]
36. Wang D, Sun X, and Sadee W (2007). Different effects of opioid antagonists on mu-, delta-, and kappa-opioid receptors with and without agonist pretreatment. J Pharmacol Exp Ther 321, 544–552. [PubMed: 17267582]
37. Knight ZA, Tan K, Birsoy K, Schmidt S, Garrison JL, Wysocki RW, Emiliano A, Ekstrand MI, and Friedman JM (2012). Molecular profiling of activated neurons by phosphorylated ribosome capture. Cell 151, 1126–1137. [PubMed: 23178128]
38. Cavicchini E, Candeletti S, Spampinato S, and Ferri S (1989). Hypothermia elicited by some prodynorphin-derived peptides: opioid and non-opioid actions. Neuropeptides 14, 45–50. [PubMed: 2571107]
39. Minor RK, Chang JW, and de Cabo R (2009). Hungry for life: How the arcuate nucleus and neuropeptide Y may play a critical role in mediating the benefits of calorie restriction. Mol Cell Endocrinol 299, 79–88. [PubMed: 19041366]
40. Atasoy D, Betley JN, Su HH, and Sternson SM (2012). Deconstruction of a neural circuit for hunger. Nature 488, 172–177. [PubMed: 22801496]
41. Gao Q, and Horvath TL (2007). Neurobiology of feeding and energy expenditure. Annu Rev Neurosci 30, 367–398. [PubMed: 17506645]
42. Yahiro T, Kataoka N, Nakamura Y, and Nakamura K (2017). The lateral parabrachial nucleus, but not the thalamus, mediates thermosensory pathways for behavioural thermoregulation. Sci Rep 7, 5031. [PubMed: 28694517]
43. Palmiter RD (2018). The Parabrachial Nucleus: CGRP Neurons Function as a General Alarm. Trends Neurosci 41, 280–293. [PubMed: 29703377]
44. Nakamura K (2011). Central circuitries for body temperature regulation and fever. Am J Physiol Regul Integr Comp Physiol 301, R1207–1228. [PubMed: 21900642]
45. Geerling JC, Kim M, Mahoney CE, Abbott SB, Agostinelli LJ, Garfield AS, Krashes MJ, Lowell BB, and Scammell TE (2016). Genetic identity of thermosensory relay neurons in the lateral

parabrachial nucleus. Am J Physiol Regul Integr Comp Physiol 310, R41–54. [PubMed: 26491097]

46. Morrison SF, and Nakamura K (2019). Central Mechanisms for Thermoregulation. Annu Rev Physiol 81, 285–308. [PubMed: 30256726]
47. Morrison SF (2016). Central control of body temperature. F1000Res 5.
48. Bouret SG, Draper SJ, and Simerly RB (2004). Formation of projection pathways from the arcuate nucleus of the hypothalamus to hypothalamic regions implicated in the neural control of feeding behavior in mice. J Neurosci 24, 2797–2805. [PubMed: 15028773]
49. Bodnar RJ (2008). Endogenous opiates and behavior: 2007. Peptides 29, 2292–2375. [PubMed: 18851999]
50. Benamar K, McMenamin M, Geller EB, Chung YG, Pintar JE, and Adler MW (2005). Unresponsiveness of mu-opioid receptor knockout mice to lipopolysaccharide-induced fever. Br J Pharmacol 144, 1029–1031. [PubMed: 15700026]
51. Chen ZC, Kuo JR, Huang YP, and Lin MT (2005). Mu-opioid receptor blockade protects against circulatory shock and cerebral ischemia during heatstroke. J Cardiovasc Pharmacol 46, 754–760. [PubMed: 16306798]
52. Colman AS, and Miller JH (2002). mu-1 opioid receptor stimulation decreases body temperature in conscious, unrestrained neonatal rats. Exp Biol Med (Maywood) 227, 377–381. [PubMed: 12037126]
53. Handler CM, Geller EB, and Adler MW (1992). Effect of mu-, kappa-, and delta-selective opioid agonists on thermoregulation in the rat. Pharmacol Biochem Behav 43, 1209–1216. [PubMed: 1361992]
54. Handler CM, Piliero TC, Geller EB, and Adler MW (1994). Effect of ambient temperature on the ability of mu-, kappa- and delta-selective opioid agonists to modulate thermoregulatory mechanisms in the rat. J Pharmacol Exp Ther 268, 847–855. [PubMed: 8113997]
55. Mayfield KP, and D'Alecy LG (1992). Role of endogenous opioid peptides in the acute adaptation to hypoxia. Brain Res 582, 226–231. [PubMed: 1393544]
56. Romanovsky AA, and Blatteis CM (1996). Heat stroke: opioid-mediated mechanisms. J Appl Physiol (1985) 81, 2565–2570. [PubMed: 9018507]
57. Scarpellini Cda S, Gargaglioni LH, Branco LG, and Bicego KC (2009). Role of preoptic opioid receptors in the body temperature reduction during hypoxia. Brain Res 1286, 66–74. [PubMed: 19545549]
58. Spencer RL, Hruby VJ, and Burks TF (1988). Body temperature response profiles for selective mu, delta and kappa opioid agonists in restrained and unrestrained rats. J Pharmacol Exp Ther 246, 92–101. [PubMed: 2839673]
59. Steiner AA, Rocha MJ, and Branco LG (2002). A neurochemical mechanism for hypoxia-induced anapyrexia. Am J Physiol Regul Integr Comp Physiol 283, R1412–1422. [PubMed: 12388478]
60. Salmi P, Kela J, Arvidsson U, and Wahlestedt C (2003). Functional interactions between delta- and mu-opioid receptors in rat thermoregulation. Eur J Pharmacol 458, 101–106. [PubMed: 12498912]
61. Spencer RL, Hruby VJ, and Burks TF (1990). Alteration of thermoregulatory set point with opioid agonists. J Pharmacol Exp Ther 252, 696–705. [PubMed: 2313595]
62. Xin L, Geller EB, and Adler MW (1997). Body temperature and analgesic effects of selective mu and kappa opioid receptor agonists microdialyzed into rat brain. J Pharmacol Exp Ther 281, 499–507. [PubMed: 9103537]
63. Yakimova KS, Sann H, and Pierau FK (1996). Neuronal basis for the hyperthermic effect of mu-opioid agonists in rats: decrease in temperature sensitivity of warm-sensitive hypothalamic neurons. Neurosci Lett 218, 115–118. [PubMed: 8945741]
64. Yakimova KS, Sann H, and Pierau FK (1998). Effects of kappa and delta opioid agonists on activity and thermosensitivity of rat hypothalamic neurons. Brain Res 786, 133–142. [PubMed: 9554984]
65. Benamar K, Xin L, Geller EB, and Adler MW (2000). Blockade of lipopolysaccharide-induced fever by a mu-opioid receptor-selective antagonist in rats. Eur J Pharmacol 401, 161–165. [PubMed: 10924921]

66. Benamar K, Geller EB, and Adler MW (2002). Effect of a mu-opioid receptor-selective antagonist on interleukin-6 fever. Life Sci 70, 2139–2145. [PubMed: 12002806]

67. Geller EB, Hawk C, Tallarida RJ, and Adler MW (1982). Postulated thermoregulatory roles for different opiate receptors in rats. Life Sci 31, 2241–2244. [PubMed: 6298520]

68. Geller EB, Hawk C, Keinath SH, Tallarida RJ, and Adler MW (1983). Subclasses of opioids based on body temperature change in rats: acute subcutaneous administration. J Pharmacol Exp Ther 225, 391–398. [PubMed: 6842402]

69. Benamar K, Yondorf M, Barreto VT, Geller EB, and Adler MW (2007). Deletion of mu-opioid receptor in mice alters the development of acute neuroinflammation. J Pharmacol Exp Ther 323, 990–994. [PubMed: 17898318]

70. Rawls SM, and Benamar K (2011). Effects of opioids, cannabinoids, and vanilloids on body temperature. Front Biosci (Schol Ed) 3, 822–845. [PubMed: 21622235]

71. Leibel RL, Rosenbaum M, and Hirsch J (1995). Changes in energy expenditure resulting from altered body weight. N Engl J Med 332, 621–628. [PubMed: 7632212]

72. Landsberg L, Young JB, Leonard WR, Linsenmeier RA, and Turek FW (2009). Is obesity associated with lower body temperatures? Core temperature: a forgotten variable in energy balance. Metabolism 58, 871–876. [PubMed: 19375759]

73. Landsberg L (2012). Core temperature: a forgotten variable in energy expenditure and obesity? Obes Rev 13 Suppl 2, 97–104. [PubMed: 23107263]

74. Snyder LM, Chiang MC, Loeza-Alcocer E, Omori Y, Hachisuka J, Sheahan TD, Gale JR, Adelman PC, Sypek EI, Fulton SA, et al. (2018). Kappa Opioid Receptor Distribution and Function in Primary Afferents. Neuron 99, 1274–1288 e1276. [PubMed: 30236284]

75. Ivanisevic J, Stauch KL, Petrascheck M, Benton HP, Epstein AA, Fang M, Gorantla S, Tran M, Hoang L, Kurczy ME, et al. (2016). Metabolic drift in the aging brain. Aging (Albany NY) 8, 1000–1020. [PubMed: 27182841]

76. Tautenhahn R, Patti GJ, Rinehart D, and Siuzdak G (2012). XCMS Online: a web-based platform to process untargeted metabolomic data. Anal Chem 84, 5035–5039. [PubMed: 22533540]

77. Schymanski EL, Jeon J, Gulde R, Fenner K, Ruff M, Singer HP, and Hollender J (2014). Identifying small molecules via high resolution mass spectrometry: communicating confidence. Environ Sci Technol 48, 2097–2098. [PubMed: 24476540]

78. Sumner LW, Amberg A, Barrett D, Beale MH, Beger R, Daykin CA, Fan TW, Fiehn O, Goodacre R, Griffin JL, et al. (2007). Proposed minimum reporting standards for chemical analysis Chemical Analysis Working Group (CAWG) Metabolomics Standards Initiative (MSI). Metabolomics 3, 211–221. [PubMed: 24039616]

79. Gore BB, Soden ME, and Zweifel LS (2013). Manipulating gene expression in projection-specific neuronal populations using combinatorial viral approaches. Curr Protoc Neurosci 65, 4 35 31–20. [PubMed: 25429312]

80. Cintron-Colon R, Shankar K, Sanchez-Alavez M, and Conti B (2019). Gonadal hormones influence core body temperature during calorie restriction. Temperature (Austin) 6, 158–168. [PubMed: 31286026]

81. Jarosz PA (2007). The effect of kappa opioid receptor antagonism on energy expenditure in the obese Zucker rat. Biol Res Nurs 8, 294–299. [PubMed: 17456590]

82. Conti B, Sanchez-Alavez M, Winsky-Sommerer R, Morale MC, Lucero J, Brownell S, Fabre V, Huitron-Resendiz S, Henriksen S, Zorrilla EP, et al. (2006). Transgenic mice with a reduced core body temperature have an increased life span. Science 314, 825–828. [PubMed: 17082459]

Highlights

- Calorie restriction (CR) causes hypothermia and elevates leu-enkephalin
- Activation of prodynorphin neurons lowers temperature
- Inhibition of kappa opioid receptor (KOR) neurons reduces CR-induced hypothermia
- Blocking KOR halts CR-induced hypothermia promoting weight loss during dieting

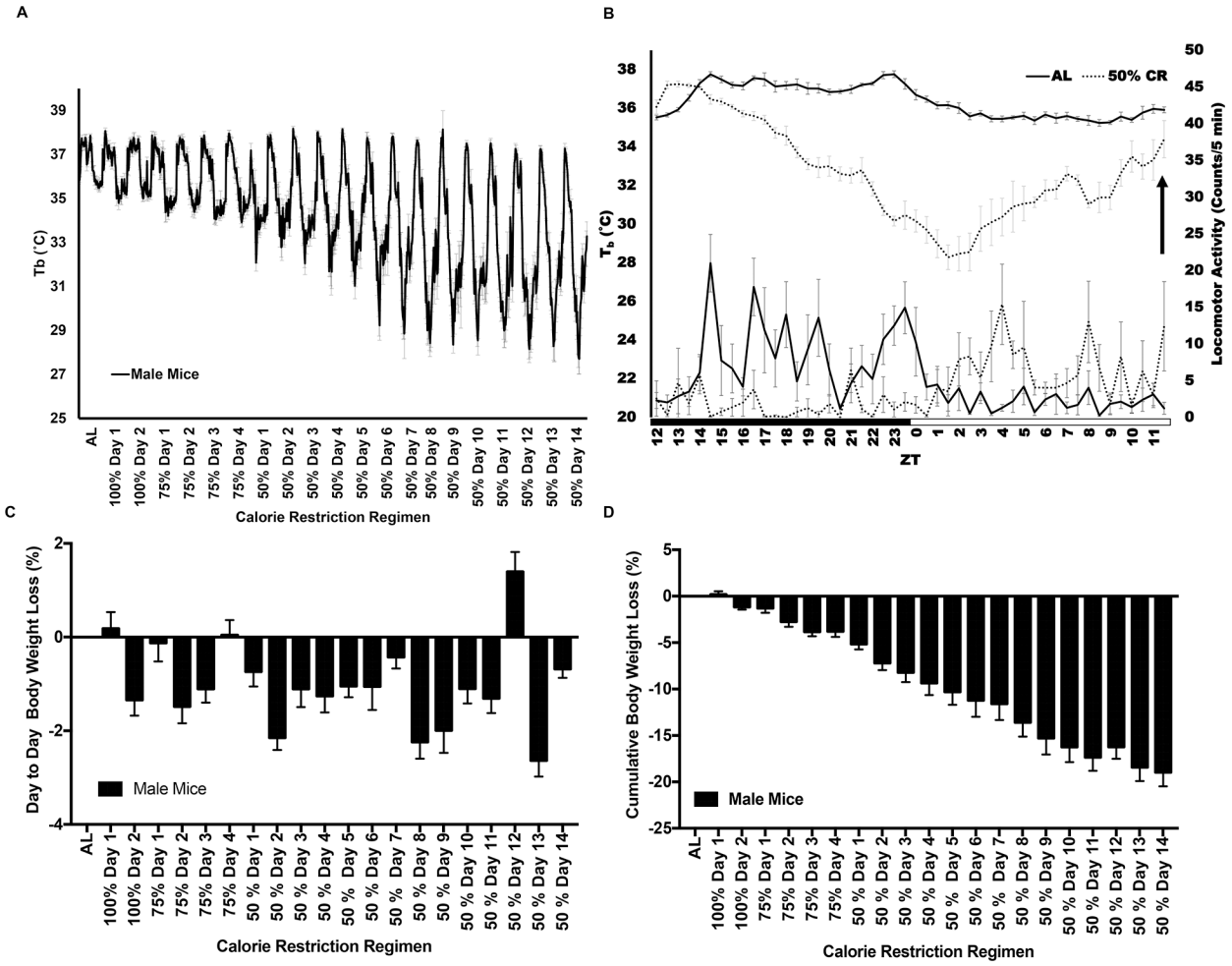

Figure 1. Body temperature and body weight are progressively reduced during calorie restriction until reaching plateau.

(**A**) T_b profile of C57BL/6 male mice from *ad libitum* to 50% CR. (**B**) Detailed 24 h T_b and locomotor activity profiles during *ad libitum* and 50% CR at day 13; black arrow indicates time in which food was given during CR. (**C**) Daily and cumulative (**D**) body weight loss percentages of C57BL/6 male mice subjected to CR. (**A-D**) n= 6 mice; graphs show mean ± SEM. (**A**) The progressive reduction in T_b was analyzed by One-way ANOVA, $R^2 = 0.3637$; $F(20, 967) = 27.64$, $P < 0.0001$, followed by posttest for linear trend, slope = −0.24, $P < 0.0001$. (**C**) RM one-way ANOVA between days of the CR regimen $F(4.486,22.43) = 16.53$, $P < 0.0001$; followed by Tukey's multiple comparisons test $P < 0.05$. (**D**) The reduction in body weight over time was analyzed by RM one-way ANOVA, $R^2 = 0.7606$; $F(1, 260) = 6127$, $P<0.0001$ followed by posttest for linear trend, slope = −0.49, $P < 0.001$. For the experimental design see Figure S1.

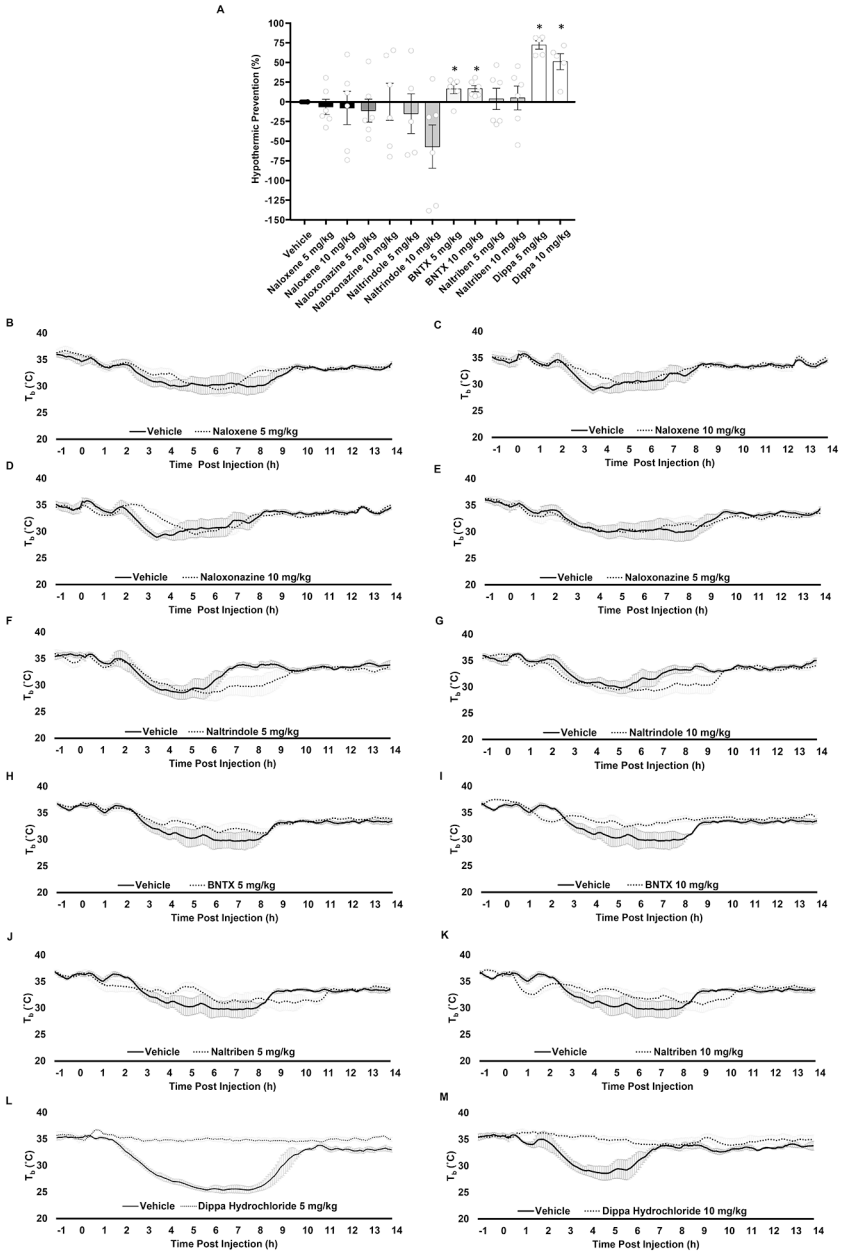

Figure 2. Opioid receptors modulate the hypothermic response to calorie restriction.

(**A**) Percentage reduction of the hypothermic response to 50% calorie restriction for each opioid receptor antagonist at different doses. (**B-M**) T_b profile of calorie restricted mice intraperitoneally administered with nonselective and selective antagonists for the opioid receptors and their respective vehicles. Nonselective antagonist Naloxene injected at time (0) at (**B**) 5 mg/kg and (**C**) 10 mg/kg. Selective μ_1 opioid receptor antagonist Naloxonazine injected at time (0) at (**D**) 5 mg/kg and (**E**) 10 mg/kg. Selective antagonist for ∂ opioid receptor Naltrindole injected at time (0) at (**F**) 5 mg/kg and (**G**) 10 mg/kg. Selective antagonist for ∂_1 opioid receptor BNTX injected at time (0) at (**H**) 5 mg/kg and (**I**) 10 mg/kg. Selective antagonist for ∂_2 opioid receptor Naltriben injected at time (0) at (**J**) 5 mg/kg and (**K**) 10 mg/kg. Selective antagonist for κ opioid receptor Dippa Hydrochloride

injected at time (0) at (**L**) 5 mg/kg and (**M**) 10 mg/kg. The percentage by which each individual antagonist reduced the hypothermic response to CR and statistical analysis were calculated as stated in the methods and presented in Figure 2A. n= 4 to 7 mice per treatment; graphs show mean ± SEM. One sample t-test, opioid receptor antagonist compared to Vehicle group, *P < 0.05. The binding affinities of the antagonists used is listed in Table S1.

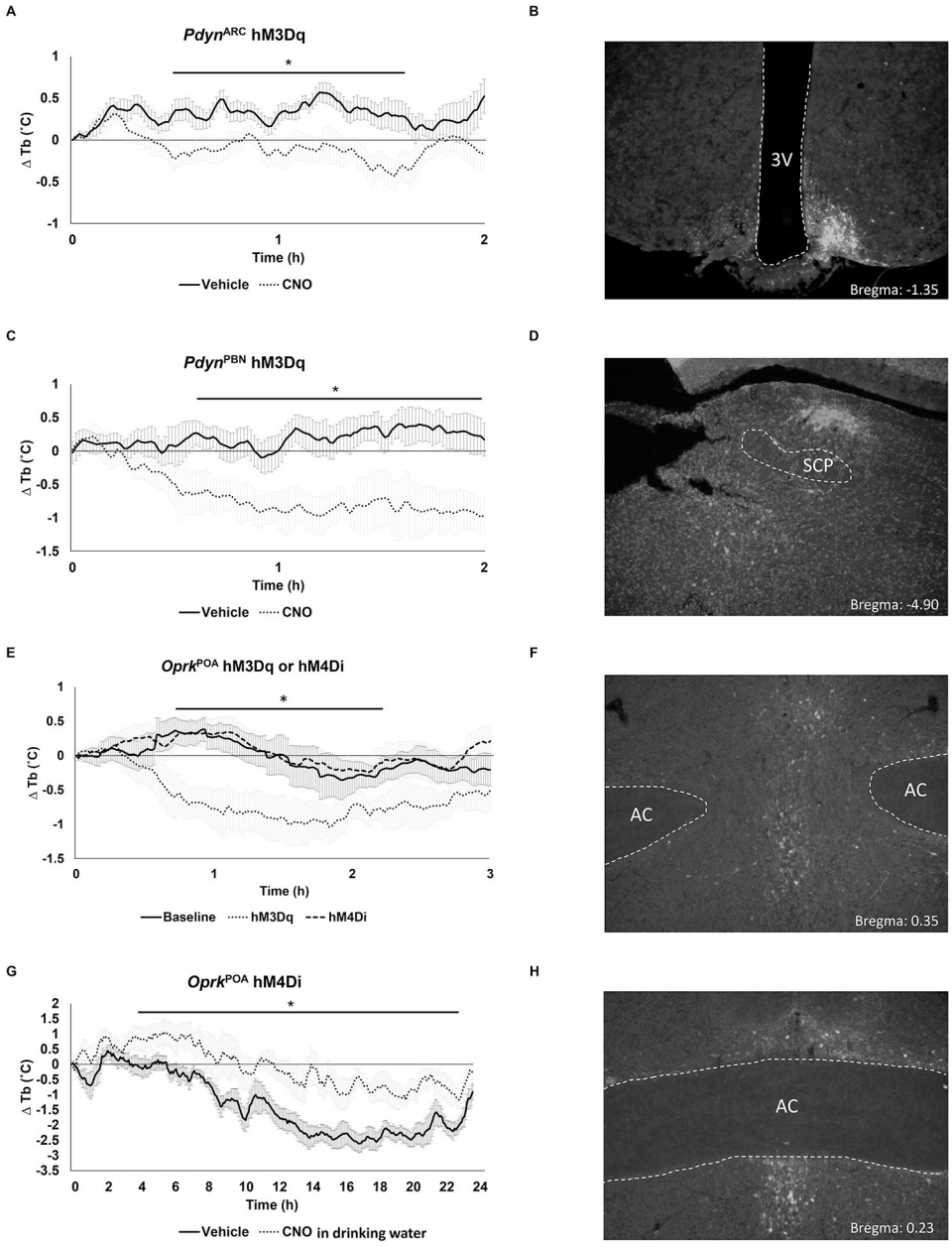

Figure 3. Effects of chemogenetic manipulation of the opioid system on body temperature.

Change in T_b response upon chemogenetic activation (hM3Dq) of Pdyn-expressing neurons in the ARC (**A**) or PBN (**C**) during *ad libitum* feeding. (**E**) Change in T_b response upon chemogenetic activation (hM3Dq) or inhibition (hM4Di) of *Oprk*-expressing neurons in the POA during *ad libitum*. (**G**) Change in T_b response upon chemogenetic inhibition of *Oprk*-expressing neurons in the POA during CR. (**A, C, E and G**) n = 6 mice per treatment; graphs show mean ± SEM. Two-way RM ANOVA followed by Sidak's or Dunnett's multiple comparisons test. (**B, D, F and H**) Representative images showing viral placement for each targeted region are shown. SCP, superior cerebellar peduncle; AC, anterior commissure; 3V, 3rd ventricle. (**A**) F(1, 10)=6.365 P =0.0302 between treated groups; Sidak's *P < 0.05. (**C**) F(1, 10)=7.247, P =0.0226 between treated groups; Sidak's *P <

0.05. (**E**) F (2, 15) = 6.099 P = 0.01; Dunnett's *P < 0.05, baseline vs hM3Dq. (**G**) F(1, 10)=11.22, P =0.0074 between treated groups; Sidak's *P < 0.05. Dippa Hydrochloride did not alter T_b in animals fed *ad libitum* (Figure S2).

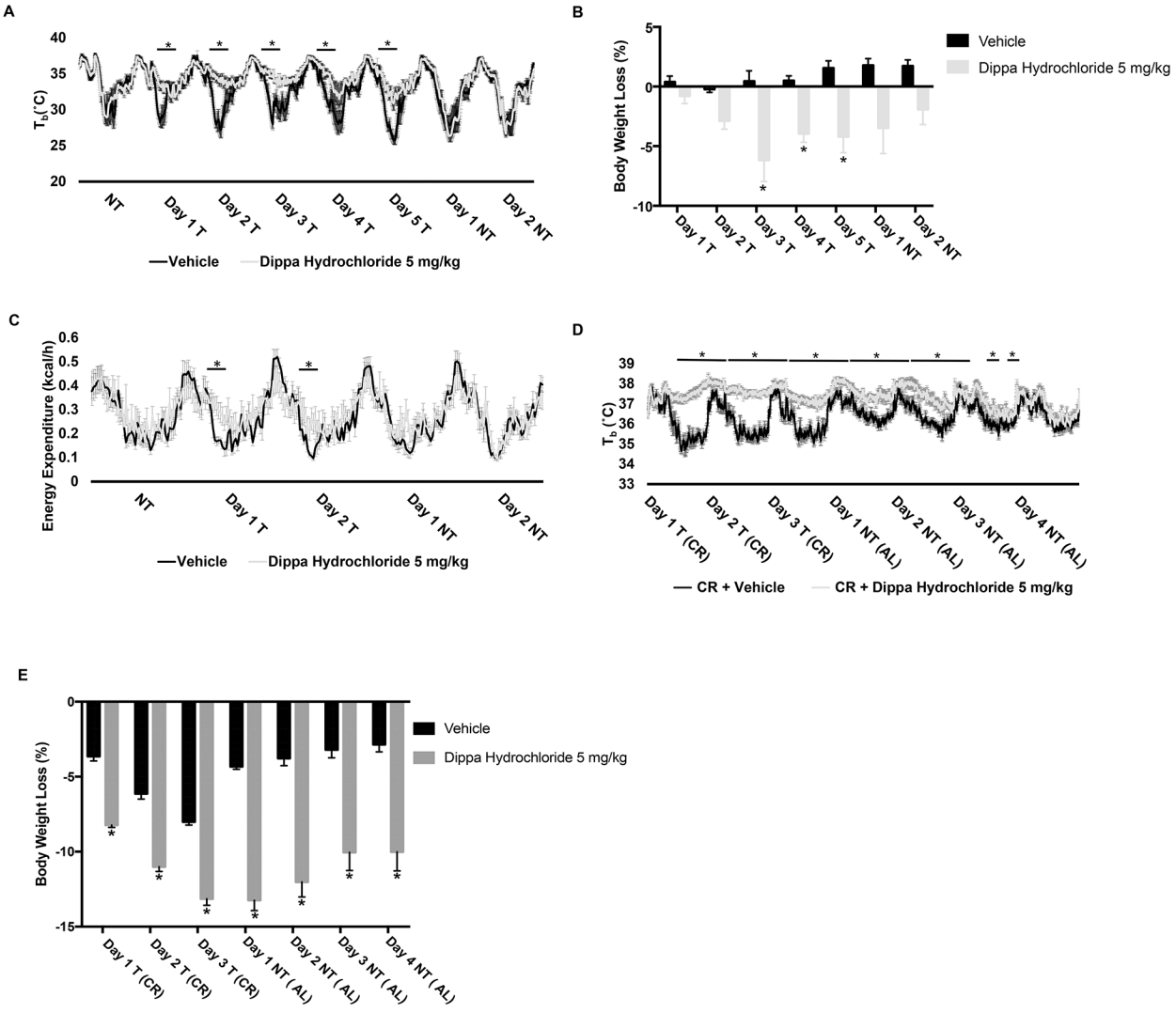

Figure 4. KOR antagonism promotes body weight loss during calorie restriction and obesity.

(**A**) T_b profile, (**B**) percentage of body weight loss and (**C**) energy expenditure of lean mice on 50% CR, before, during and after administration of DH or Vehicle. (**D**) T_b profile (**E**) percentage of body weight loss. (**A-E**) n= 6 mice per treatment; graphs show mean ± SEM. Tb. energy expenditure and body weight differences between treatments were analyzed by two-way ANOVA followed by Sidak's multiple comparisons test (**A**) F (4, 50) = 100.8, P <0.0001; Sidak's: P <0.0005 each day on treatment. (**B**) F(1, 10) = 13.77, P = 0.0040; Sidak's: P < 0.03 each day on treatment. (**C**) F (1, 20) = 15.35 P = 0.0009; Sidak's: *P <0.05 each day on treatment. (**D**) F (1, 63) = 270.4, P <0.0001; Sidak's: *P <0.05 for specific time-points between groups. (**E**) F(1, 10) = 97.31, P < 0.0001; Sidak's: P < 0.0001 each day. Abbreviations: T: treatment, NT: no treatment, CR: calorie restriction and AL: *ad libitum*. The effects of Dippa Hydrochloride on food intake are shown in Figure S3.

KEY RESOURCES TABLE

REAGENT or RESOURCE	SOURCE	IDENTIFIER
Antibodies		
Chicken anti-GFP	Abcam	Cat# ab13970; RRID: AB_300798
Rabbit anti-DsRed	Clontech	Cat# 632496; RRID: AB_10013483
Bacterial and Virus Strains		
AAV1-Ef1a-DIO-hM3:YFP	HHMI, University of Washington, Dr. R. Palmiter	N/A
AAV1-Ef1a-DIO-hM4:mCh	HHMI, University of Washington, Dr. R. Palmiter	N/A
AAV1-Ef1a-DIO-mCh	HHMI, University of Washington, Dr. R. Palmiter	N/A
Biological Samples		
Chemicals, Peptides, and Recombinant Proteins		
Naloxone hydrochloride	Tocris	Cat # 0599
Naloxonazine dihydrochloride	Tocris	Cat # 0591
Naltrindole hydrochloride	Tocris	Cat # 0740
BNTX maleate	Tocris	Cat # 0899
Naltriben mesylate	Tocris	Cat # 0892
DIPPA hydrochloride	Tocris	Cat # 0794
0.1% Formic acid in acetonitrile	Honeywell	LC441–2.5
0.1% Formic acid in water	Honeywell	LC452–2.5
Critical Commercial Assays		
Deposited Data		
mzXML files	XCMS Online	https://xcmsonline.scripps.edu
Analyzed data	This paper	
Experimental Models: Cell Lines		
Experimental Models: Organisms/Strains		

REAGENT or RESOURCE	SOURCE	IDENTIFIER
C57BL/6 mice	The Scripps Research Institute breeding colony	N/A
Pdyn-Cre	HHMI, University of Washington, Dr. R. Palmiter	N/A
KOR-Cre	University of Pittsburgh, Dr. S. Ross	N/A
Oligonucleotides		
Recombinant DNA		
Software and Algorithms		
Excel	Microsoft	https://products.office.com/en-us/excel
GraphPad Prism 7	GraphPadSoftware	https://www.graphpad.com/
XCMX Online	https://doi.org/10.1021/ac300698c	https://xcmsonline.scripps.edu/
Telemetry	Starr Life Sciences	G2 E-Mitters
Telemetry	Data Sciences, Inc	TA10TA-F10
Telemetry analysis	Vital view	https://www.starrlifesciences.com/products/vitalview-software
Other		
Normal Chow	Lab Diet	5053 Irradiated Pico Lab
High Fat Diet	Research Diets	D12492
Acquity UPLC I-class	Waters	ACQUITY UPLC I-Class PLUS System
Synapt G2-Si	Waters	SYNAPT G2-Si High Definition Mass Spectrometry
ACQUITY UPLC BEH C18 Column, 130Å, 1.7 µm, 2.1 mm X 100 mm	Waters	186002352
LCMS Certified Clear Glass 12 × 32mm Screw Neck Vial, with Cap and Preslit PTFE/Silicone Septa, 2 mL Volume	Waters	600000668CV